www.nature.com/aps

Acta Pharmacologica Sinica

ARTICLE

Cinnamaldehyde protects against rat intestinal ischemia/reperfusion injuries by synergistic inhibition of NF-κB and p53

Marwan Almoiliqy[1], Jin Wen[1], Bin Xu[1], Yu-chao Sun[1], Meng-qiao Lian[1], Yan-li Li[1], Eskandar Qaed[1], Mahmoud Al-Azab[1], Da-peng Chen[2], Abdullah Shopit[1], Li Wang[1], Peng-yuan Sun[1] and Yuan Lin[1]

Our preliminary study shows that cinnamaldehyde (CA) could protect against intestinal ischemia/reperfusion (I/R) injuries, in which p53 and NF-κB p65 play a synergistic role. In this study, we conducted in vivo and in vitro experiments to verify this proposal. SD rats were pretreated with CA (10 or 40 $mg \cdot kg^{-1} \cdot d^{-1}$, ig) for 3 days, then subjected to 1 h mesenteric ischemia followed by 2 h reperfusion. CA pretreatment dose-dependently ameliorated morphological damage and reduced inflammation evidenced by decreased TNF-α, IL-1β, and IL-6 levels and MPO activity in I/R-treated intestinal tissues. CA pretreatment also attenuated oxidative stress through restoring SOD, GSH, LDH, and MDA levels in I/R-treated intestinal tissues. Furthermore, CA pretreatment significantly reduced the expression of inflammation/apoptosis-related NF-κB p65, IKKβ, IK-α, and NF-κB p50, and downregulated apoptotic protein expression including p53, Bax, caspase-9 and caspase-3, and restoring Bcl-2, in I/R-treated intestinal tissues. We pretreated IEC-6 cells in vitro with CA for 24 h, followed by 4 h hypoxia and 3 h reoxygenation (H/R) incubation. Pretreatment with CA (3.125, 6.25, and 12.5 $\mu mol \cdot L^{-1}$) significantly reversed H/R-induced reduction of IEC-6 cell viability. CA pretreatment significantly suppressed oxidative stress, NF-κB activation and apoptosis in H/R-treated IEC-6 cells. Moreover, CA pretreatment significantly reversed mitochondrial dysfunction in H/R-treated IEC-6 cells. CA pretreatment inhibited the nuclear translocation of p53 and NF-κB p65 in H/R-treated IEC-6 cells. Double knockdown or overexpression of p53 and NF-κB p65 caused a synergistic reduction or elevation of p53 compared with knockdown or overexpression of p53 or NF-κB p65 alone. In H/R-treated IEC-6 cells with double knockdown or overexpression of NF-κB p65 and p53, CA pretreatment caused neither further decrease nor increase of NF-κB p65 or p53 expression, suggesting that CA-induced synergistic inhibition on both NF-κB and p53 played a key role in ameliorating intestinal I/R injuries. Finally, we used immunoprecipitation assay to demonstrate an interaction between p53 and NF-κB p65, showing the basis for CA-induced synergistic inhibition. Our results provide valuable information for further studies.

Keywords: cinnamaldehyde; mesenteric ischemia/reperfusion injury; inflammation; oxidative stress; apoptosis; mitochondria; p53; NF-κB

Acta Pharmacologica Sinica (2020) 41:1208–1222; https://doi.org/10.1038/s41401-020-0359-9

INTRODUCTION

The common denominators of diverse I/R-induced tissue injuries, including cerebral, cardiac, renal, hepatic, and intestinal injuries, are found to provoke excessive inflammation, oxidative stress, and apoptosis [1–5]. Intestinal I/R injuries may induce loss of intestinal epithelial barrier function, leading to the translocation of endotoxins and bacteria to local and remote organs [6, 7] and triggering the release of inflammatory cytokines, the development of sepsis, and the initiation of systemic inflammatory response syndrome and multiple organ dysfunction syndrome [8–10].

Multiple targets, including MAPK, MEK, ERK, PI3K, AIF, ROCK, JNK, AKT, JAK2/STAT3, p53, and NF-κB, are involved in tissue injuries [11–15]. Diverse natural compounds provide beneficial health effects through modulating these targets against excessive and/or aberrant inflammation, oxidative stress, and apoptosis [16–18]. For instance, ginsenosides ameliorate myocardial I/R-induced inflammation, oxidative stress, and apoptosis via inhibiting the p53 pathway [19]. Berberine ameliorates renal I/R-induced inflammation, mitochondrial dysfunction, oxidative stress, and apoptosis via inhibiting the p53 pathway [20]. Astaxanthin ameliorates hepatic I/R injuries by attenuating inflammation, oxidative stress, and apoptosis through modulating AKT/HIF-α/MAPK pathways [21]. 6-Gingerol attenuates myocardial I/R injuries by reducing inflammation, oxidative stress, and apoptosis through NF-κB/JNK pathways [22]. Gastrin ameliorates myocardial I/R-induced injury by modulating AKT/ERK1/2/STAT3 pathways [23]. Coptisine attenuates myocardial I/R-induced injury through RhoA/ROCK pathways [24]. Paeoniflorin ameliorates I/R-induced nerve injuries via activation of Ras/MEK/ERK [25]. Our previous studies showed that catalpol ameliorated intestinal I/R-induced injury by attenuating inflammation, oxidative stress, and apoptosis through suppressing the JAK2/STAT3 pathway [26]; myricetin attenuated intestinal I/R-induced injury by reducing inflammation, oxidative stress, and apoptosis via the p-MKK7 pathway [27]; and paeoniflorin ameliorated intestinal I/R-induced injury by reducing inflammation, oxidative stress, and

[1]Pharmaceutical College, Dalian Medical University, Dalian 116044, China and [2]Laboratory Animal Center, Dalian Medical University, Dalian 116044, China
Correspondence: Peng-yuan Sun (pysun@dmu.edu.cn) or Yuan Lin (linyuandmu2008@qq.com)
These authors contributed equally: Marwan Almoiliqy, Jin Wen, Eskandar Qaed

Received: 2 July 2019 Accepted: 2 January 2020
Published online: 1 April 2020

apoptosis and promoting autophagy through the LKB1/AMPK pathway [28].

Cinnamon is obtained from the inner bark of several tree species from the genus *Cinnamomum*. Cinnamaldehyde (CA) is a major component of cinnamon [29]. CA possesses diverse beneficial effects, including anti-bacterial [30], anti-inflammatory [31], anti-oxidative [32], and anti-apoptotic effects [33]. CA has been found to ameliorate bacterial infection [34], peptic ulcers [35], diabetes [36], cardiac hypertrophy [37], myocardial I/R [38], and cerebral I/R injuries [39]. However, whether CA can effectively ameliorate intestinal I/R injuries remains to be clarified. Based on our preliminary experiments, we proposed that CA could protect against intestinal I/R injuries by attenuating inflammation, oxidative stress, mitochondrial dysfunction, and apoptosis, and CA-induced synergistic inhibition of both NF-κB and p53 played a key role in the amelioration. Rats with intestinal I/R injuries and a hypoxia/reoxygenation (H/R)-injured intestinal epithelial cell line (IEC-6 cells) were used to verify our hypothesis.

MATERIALS AND METHODS

Chemicals and materials

Cinnamaldehyde (purity: ≥98%) was purchased from Aladdin. Reagent kits for detecting superoxide dismutase, glutathione, malondialdehyde (MDA), lactate dehydrogenase (LDH), and apoptosis (via TUNEL) were obtained from Nanjing Jiancheng Institute of Biotechnology (Nanjing, China). ELISAs for measurement of tumor necrosis factor alpha (TNF-α), interleukin-1β (IL-1β), interleukin-6 (IL-6), and myeloperoxidase (MPO) were supplied by Shanghai Lengton Bioscience Co. LTD (Shanghai, China). Dulbecco's minimum essential medium (DMEM), nonessential amino acids, and glutamine were purchased from Gibco (CA, USA). Fetal bovine serum (FBS) was purchased from ScienCell Research Laboratories (CA, USA). Protein extraction kits and bicinchoninic acid (BCA) protein assay kits were obtained from Beyotime Institute of Biotechnology (Jiangsu, China). Cell counting kit-8 (CCK-8) was provided by Biotool (Shanghai, China). siRNAs against NF-κB p65 and p53 as well as Lipofectamine 2000 were provided by GenePharma (Shanghai, China). cDNA of NF-κB p65 and p53 were provided by Genecopia (Guangzhou, China). Protein A + G agarose was provided by Beyotime Institute of Biotechnology (Jiangsu, China). A rat small intestinal crypt epithelial cell line (IEC-6 cells) was purchased from American Type Culture Collection (ATCC). Other materials, including 4′, 6-diamidino-2-phenylindole (DAPI), pyruvate, glutamate, malate, succinate, cytochrome *c*, rotenone, oligomycin, FFCP, digitonin, antimycin-A, and ADP, were provided by Sigma-Aldrich (St Louis, MO, USA). All other reagents were used at an analytical grade.

Animals

Male Sprague-Dawley rats (200–220 g) were provided by the Experimental Animal Center, Dalian Medical University (Certificate of Conformity: NO. SCXK (Liao) 2008–2002). All experimental protocols were strictly conducted in conformity with the National Institutes of Health Guide for Care and Use of Laboratory Animals (Publication no. 85-23, revised 1985) and the Dalian Medical University Animal Care and Ethics Committee (Approval number: L20140402). The animal protocol was designed to minimize pain and discomfort to the animals. Rats were housed one per cage in a controlled environment with alternating 12 h light/dark cycles. Rats were deprived of food for 12 h before the experiments.

Intestinal I/R model establishment

A rat model of I/R injury to the small intestines was established as previously described [40]. After one week of housing and before inducing I/R injuries, rats were fasted with free access to water for 12 h. Then, rats were subjected to an abdominal incision (approximately 2 cm midline) after anesthetization with intraperitoneal (ip) administration of pentobarbital (50 mg/kg). The superior mesenteric artery (SMA) was exposed and occluded with a traumatic microvascular clamp for 1 h to induce ischemia. Then, the clamps were removed, and the skin was sutured to begin reperfusion for the next 2 h [26, 27]. After reperfusion, the rats were euthanized, and all serum samples were collected for further analysis. Intestinal tissues of the jejunum were collected and placed on ice, rinsed with physiological saline and were stored at −80 °C. Parts of jejunal segments were fixed with formalin for IHC, TUNEL, and histological analysis [41].

Rats were randomly assigned into five groups ($n = 5$ in each group): sham group: vehicle was administered via intragastric gavage (ig) for three days before sham surgery; (2) sham + CA (H) group: animals were administered CA (40 mg/kg, ig) once daily for three days before sham surgery; (3) I/R group: animals were subjected to 1 h of intestinal ischemia and 2 h of reperfusion after being given a vehicle ig for three consecutive days; (4) I/R + CA (L) group: animals were pretreated with CA (10 mg/kg, ig) once daily for three days before the I/R surgery; and (5) I/R + CA (H) group: animals were pretreated with CA (40 mg/kg, ig) once daily for three days before the I/R surgery. Cinnamaldehyde was suspended in 1% carboxymethyl cellulose (CMC) and was suitable for oral gavage administration at 2 mL/kg.

Histological examination

Isolated intestinal segments were fixed in a 4% paraformaldehyde solution and then were embedded in paraffin; the tissue was then cut into 4-μm slices using a sectioning apparatus (LEICA, RM2245, Germany). Staining was performed with hematoxylin and eosin (H&E) according to the manufacturer's instructions. The samples were selected randomly. The extent of I/R-induced injuries was evaluated according to Chiu's score [42].

Biochemical analysis

Rat jejunal homogenate samples were collected after tissue homogenization in saline at 4 °C and were then centrifuged at 3000 g/min for 10 min at 4 °C. Levels of tissue proinflammatory cytokines, TNF-α, IL-1β, IL-6, and MPO, were determined using enzyme-linked immunosorbent assay kits according to the manufacturer's instructions (Lengton, Shanghai, China). The levels of SOD, GSH, LDH, and MDA (Nanjing Jiancheng, China) were measured using commercial kits according to the manufacturer's instructions.

Cell culture and hypoxia/reoxygenation (H/R) incubation

IEC-6 cells were cultured according to the supplier recommendations. IEC-6 cells were cultured in DMEM supplemented with 10% fetal bovine serum, 1% penicillin/streptomycin, and 0.1 U/mL bovine insulin as described [27]. To induce hypoxia, IEC-6 cells were incubated for 4 h in a humidified hypoxic chamber (Thermo, Waltham, MA) that contained 5% CO_2 and 1% O_2 and was balanced with 94% N_2, and then the cells were cultured in normoxic conditions for an additional 3 h to achieve reoxygenation. IEC-6 cells were pretreated with CA or with the same volume of a vehicle solution 24 h prior to H/R induction.

Cell viability assay

IEC-6 cells were seeded in 96-well plates at a concentration of 1×10^4 cells per well in 100 μL of DMEM, and they were grown overnight. After that, cells were treated with various dilutions of CA (1.56, 3.125, 6.25, 12.5, and 50 $\mu mol \cdot L^{-1}$), and the cells were then incubated at 37 °C with 5% CO_2 for 24 h before H/R induction. Ten microliters of CCK-8 reagent was added to each well for 1 h incubation at 37 °C, and then absorbance readings were obtained at 450 nm using a microplate reader (Enspire2300).

Measurement of mitochondrial function

Mitochondrial respiration activity was detected by using high resolution respirometry (HRR; Oxygraph-2k, Oroboros, Innsbruck,

Austria) for respiration measurement. All chemicals were prepared, adjusted and stored according to the manufacturer's instructions. For intact and permeabilized cells, IEC-6 cell suspensions (2 mL) were added to oxygraph-2 chambers, and chemicals were added as described according to the instructions [43, 44].

Immunohistochemistry analysis

Immunohistochemistry (IHC) analysis was performed to determine the protein level of NF-κB p65; sections of paraffin-embedded jejunum were dewaxed and washed with PBS, and then 3% H_2O_2 solution was added, which was followed by incubation in blocking buffer for 30 min. Jejunal sections were then incubated with polyclonal rabbit anti-rat NF-κB p65 (1:50, Proteintech, Wuhan, China) overnight and then were incubated with horseradish-conjugated goat anti-rabbit antibody (HRP) (1:50, Proteintech, Wuhan, China), which was followed by washing with PBS. Finally, tissue slides were stained with diaminobenzidine (DAB) and hematoxylin for counterstaining and were imaged using a microscope (DM4000B, Leica, Germany) [45].

cDNA amplification

Total RNA was extracted from intestinal tissues and IEC-6 cells using TRIzol reagent (Invitrogen, Carlsbad, CA). The initial cDNA was synthesized using reverse transcriptase according to the manufacturer's instructions (Nanjing Jiancheng Corp., China). A SYBR PrimeScript RT kit was used for cDNA amplification with a real-time quantitative PCR procedure as described in the manufacturer's protocol (Nanjing Jiancheng Corp., China) [46].

Immunofluorescence staining

IEC-6 cells were seeded in 24 plates and were allowed to grow overnight; CA was added to the cells for 24 h before H/R induction, and then immunofluorescence assays were performed as described [47]. Samples were washed with PBS 3 times/5 min and analyzed using fluorescence microscopy (BX63, IX81, Olympus, Japan).

ROS staining

ROS detection was performed using an ROS staining kit (DCFH-DA, Sigma-Aldrich, USA) according to the manufacturer's instructions. IEC-6 cells were seeded and grown overnight; CA was added for 24 h before H/R. Then, the cells were washed with PBS, incubated in an ROS solution at 37 °C for 20 min and analyzed using fluorescence microscopy (BX63, IX81, Olympus, Japan) [48].

Measurement of mitochondrial membrane potential

The assessment of mitochondrial membrane potential (MMP ΔΨm) was performed by using fluoroprobe 5,5′,6,6′-tetrachloro-1,1′,3,3′-tetraethylbenzimidazolocarbo-cyanine iodide (JC-1) according to the manufacturer's instructions (Invitrogen, Carlsbad, CA). IEC-6 cells were seeded in 6-well plates and treated with 3.125 and 12.5 $\mu mol \cdot L^{-1}$ CA for 24 h prior to H/R induction. Then, the cells were washed with PBS, stained with JC-1 dye (1 μg/mL) and incubated at 37 °C for 30 min in the dark; signals were then assessed using a fluorescence microscope (BX63, IX81, Olympus, Japan) [49].

Cell transfection

NF-κB p65 and/or p53 were knocked down and overexpressed in H/R-injured IEC-6 cells according to the manufacturer's instructions. IEC-6 cells were seeded in 6-well plates, and then a specific NF-κB p65 siRNA, p53 siRNA, and control siRNA (GenePharma, Shanghai, China) or a specific cDNA encoding NF-κB p65, p53, and control cDNA (Genecopia, Guangzhou, China) were transfected with Lipofectamine 2000 reagent (GenePharma, Shanghai, China). Cotransfection of NF-κB p65 and p53 siRNA or NF-κB p65 and p53 cDNA was also performed according to the manufacturer's instructions. After 48 h, CA was added to the incubation for 24 h before H/R, and then the protein levels of NF-κB p65, p53 and Bax were estimated as previously prescribed [50].

Immunoprecipitation

To determine the potential interaction between NF-κB p65 and p53, 1 μg of p53 antibody or rabbit immunoglobulin G control antibody (Proteintech, Wuhan, China) and the extracts obtained from normal IEC-6 cells, H/R-injured IEC cells, and CA + H/R-injured IEC cells were combined and stirred slowly at 4 °C overnight. On the following day, 20 μL of protein A + G agarose beads (Beyotime, Shanghai, China) was added and incubated with the mix for an additional 3 h; then, the supernatant was removed after centrifugation, and the beads were washed five times in lysis buffer. The antibody-bound complexes were eluted by boiling in 1x sodium dodecyl sulfate (SDS) sample buffer. Samples were resolved on a 10% gel by SDS-PAGE for NF-κB p65 immunoblotting [51].

TUNEL immunostaining

Tissue samples were dewaxed, incubated with 0.1% TritonX-100 for 10 min, and then washed with PBS. After washing, tissue samples were stained using a TUNEL-based apoptosis detection assay kit (Nanjing Jiancheng Corp., China) according to the manufacturer's instructions. Positive apoptotic cells were identified by fluorescence microscopy (BX63, IX81, Olympus, Japan).

Western blotting analysis

Proteins were obtained from three randomly selected individual rat intestinal tissues from each group and from three individual groups of IEC-6 cells by lysing with total protein lysis buffer (P0013, Beyotime, Shanghai, China). The supernatant was collected and quantified using a BCA kit (Beyotime, Jiangsu, China). Equivalent amounts of protein samples were loaded with loading buffer and separated on 8%, 10%, or 12% acrylamide gels according to the molecular weight of the protein of interest. The proteins were transferred for 1 h to nitrocellulose membranes (Merck Millipore, Darmstadt, Germany). The membranes were blocked with 5% skimmed milk or 5% bovine serum albumin diluted in Tris-buffered saline with Tween (TBS-T) for 1 h at 37 °C. Then, membranes were incubated with the following relevant primary antibodies overnight at 4 °C: IKKβ, IK-α, NF-κB p50, NF-κB p65, p53, Bax, Bcl-2, caspase-3, caspase-9, and SOD-2 (Proteintech, Wuhan, China). After primary antibody incubation, blots were washed three times in TBS-T and then were incubated with a horseradish-conjugated goat anti-rabbit antibody (Proteintech, Wuhan, China) at 37 °C for 1 h. Membranes were developed with an ECL detection system (Proteintech, Wuhan, China). Image Lab software (Bio-Rad, CA, USA) was used for protein quantification of three independent experiments and were normalized to the corresponding expression of β-actin. The methods for protein level determination were described previously [52, 53].

Statistical analysis

GraphPad Prism 5.0 (GraphPad Prism Software, La Jolla, CA) was used for data analysis. All values are presented as the mean ± standard deviation SD. One-way ANOVA was used to compare means between groups. *P*-values of less than 0.05 indicated statistically significant differences. Data were statistically analyzed using DatLab software (Oroboros Instruments).

RESULTS

Cinnamaldehyde-induced protective effects against I/R-induced intestinal morphological damage

H&E staining indicated that I/R-induced rat intestinal injuries possessed the following indicators of morphological damage: massive inflammatory cell infiltration characterized by denuded villi, disruption of mucosal integrity, dilated capillaries, and digestion, as well as disintegration of the lamina propria,

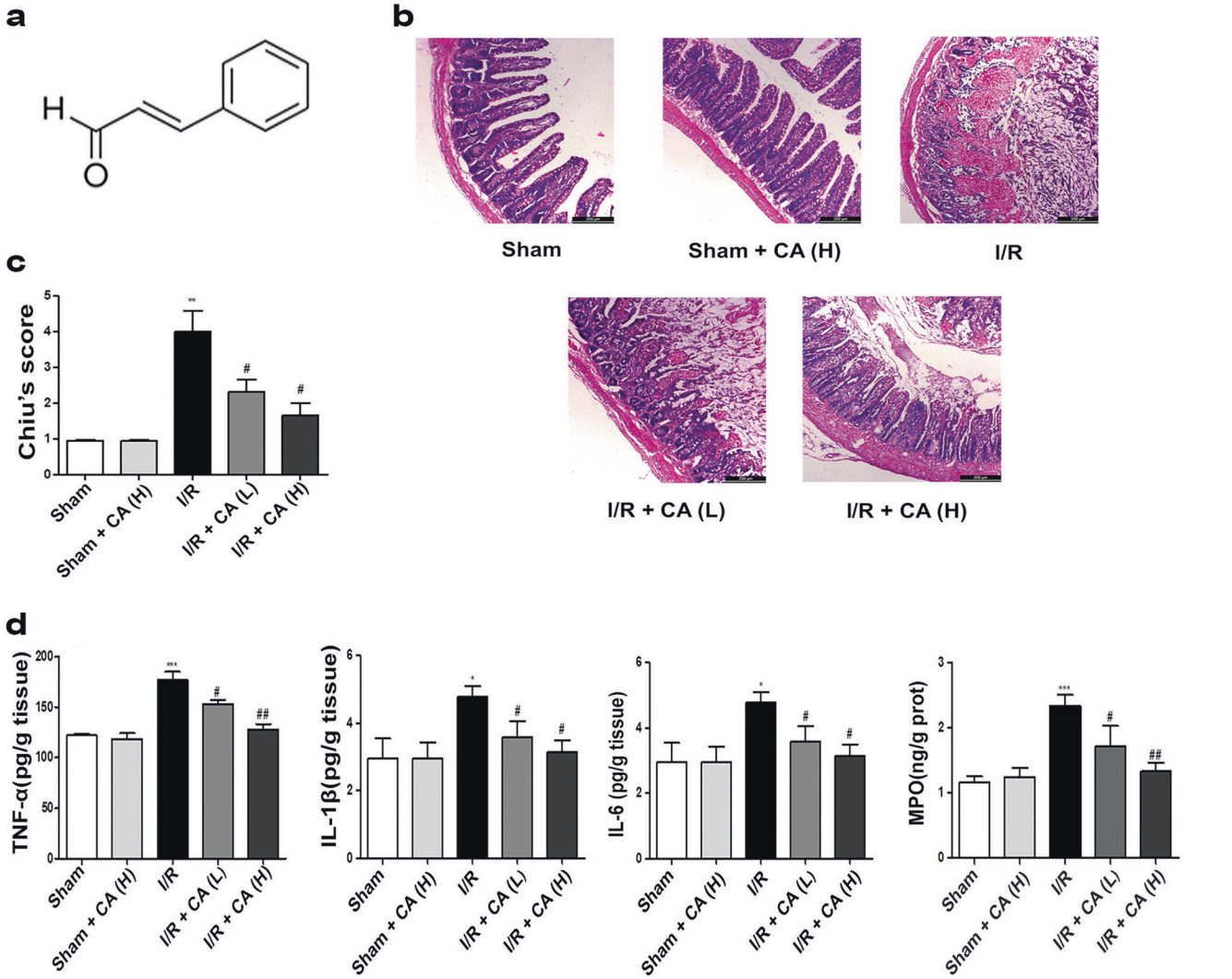

Fig. 1 Cinnamaldehyde protected against intestinal I/R-induced morphological damage and inflammation. **a** The chemical structure of cinnamaldehyde. **b** Representative images of intestinal histology (H&E staining, original magnification ×100). **c** Chiu's score of the intestine after intestinal I/R. **d** Tissue levels of TNF-α, IL-1β, IL-6 and MPO. Data are expressed as the mean ± SD ($n = 5$), $^{***}P < 0.001$, $^{**}P < 0.01$, and $^{*}P < 0.05$ vs sham group; $^{###}P < 0.001$, $^{##}P < 0.01$, and $^{#}P < 0.05$ vs I/R group

hemorrhaging, and ulceration. CA pretreatment (10 and 40 mg/kg) protected against and ameliorated I/R-induced intestinal damage (Fig. 1b). Chiu's score was significantly increased in I/R-injured rats over that of sham-operated rats, and CA pretreatment significantly reversed Chiu's score (Fig. 1c). CA did not induce a significant histological alteration in the sham-operated rats.

Cinnamaldehyde-induced protective effects against I/R-induced intestinal inflammation

The activities of pro-inflammatory cytokines, TNF-α, IL-1β, IL-6, and MPO, were significantly increased in I/R-injured intestines compared with that of sham-operated rats. CA pretreatment (10, 40 mg/kg) significantly reversed these values in a dose-dependent manner (Fig. 1d), suggesting that CA-mediated reductions of injuries were related to the inhibition of inflammation. CA did not significantly affect these parameters in sham-operated rats.

Cinnamaldehyde-induced protective effects against I/R-induced intestinal oxidative stress

The results obtained from enzymatic assays indicated that the levels of SOD and GSH were significantly reduced, and the levels of LDH and MDA were significantly elevated in intestinal I/R-injured rats compared with the levels observed in sham-operated rats. CA pretreatment significantly reversed SOD, GSH, LDH, and MDA levels in the treated I/R rats (Fig. 2a) compared with that of the I/R control rats. Western blot analysis indicated that SOD protein expression was significantly reduced in both I/R-injured rats (Fig. 2b, c) and H/R-injured IEC-6 cells (Fig. 2d, e) compared with the corresponding controls. CA pretreatment significantly reversed the decrease in SOD protein expression in I/R-injured rats and in H/R-injured IEC-6 cells (Fig. 2b-e). ROS fluorescence assays indicated a significant increase in ROS in H/R-injured IEC-6 cells compared with that of the control IEC-6 cells. CA pretreatment significantly reduced ROS generation in a dose-dependent manner (Fig. 2f), suggesting that the protective effects of CA against intestinal I/R injuries are related to the inhibition of oxidative stress. CA did not significantly affect these parameters in sham-operated rats or in control IEC-6 cells.

Cinnamaldehyde-induced reversion of the decreased cell viability

Cell Counting Kit-8 (CCK-8) assays were used to determine cell viability. The results indicated that CA in a concentration range of 1.56–50 $\mu mol \cdot L^{-1}$ did not significantly affect the viability of normal IEC-6 cells (Fig. 2g). Under H/R conditions, CA pretreatment at concentrations of 3.125, 6.25 and 12.5 $\mu mol \cdot L^{-1}$ significantly reversed the decreased viability compared with that of the control

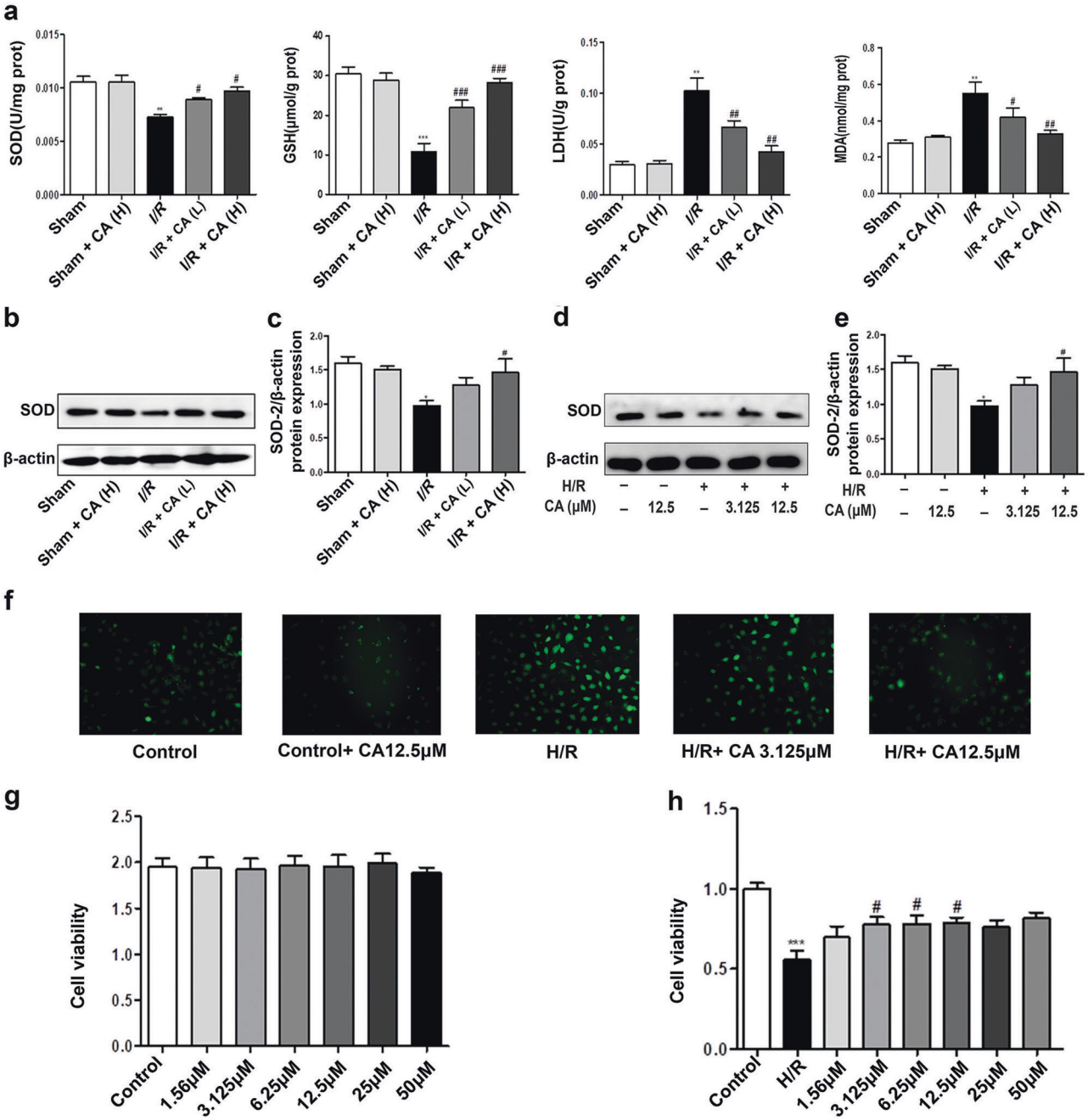

Fig. 2 Cinnamaldehyde protected against intestinal I/R- and H/R-induced oxidative stress. **a** Tissue levels of SOD, GSH, LDH, and MDA. **b** The levels of SOD protein expression in intestinal tissues from three individual samples of randomly selected rats from each group. **c** Quantification analysis of SOD in intestinal tissues is performed for three independent experiments. **d** The levels of SOD protein expression in normal/H/R-injured IEC-6 cells from three individual samples. **e** Quantification of SOD in normal/H/R-injured IEC-6 cells from three independent experiments. **f** ROS assays were performed on the IEC-6 cell line. **g** The effect of CA (1.56, 3.125, 6.25, 12.5, 25, and 50 μmol · L^{-1}) on IEC-6 cell viability for 24 h under normal conditions. **h** The effect of CA (1.56, 3.125, 6.25, 12.5, 25, and 50 μmol · L^{-1}) on IEC-6 cell viability for 24 h in H/R conditions. Data are expressed as the mean ± SD ($n = 3$), $^{***}P < 0.001$, $^{**}P < 0.01$, and $^{*}P < 0.05$ vs sham group; $^{###}P < 0.001$, $^{##}P < 0.01$, and $^{#}P < 0.05$ vs I/R group

H/R-injured IEC-6 cells (Fig. 2h), suggesting that CA-induced protection of IEC-6 cells against H/R-induced injury was related to the reversal of decreased cell viability.

Cinnamaldehyde-induced improvement of H/R-induced mitochondrial dysfunction

I/R injuries may induce mitochondrial membrane depolarization, mitochondrial respiration dysfunction, and apoptosis [54, 55]. Mitochondrial membrane permeability (MMP ΔΨm) was determined by using a JC-1 (5,5′,6,6′-tetrachloro-1,1′,3,3′-tetraethylbenzimidazolocarbo-cyanine iodide) staining assay. Our results indicated that both JC-1 aggregates and MMP were significantly decreased in H/R-injured IEC-6 cells compared with that of normal IEC-6 cells, indicating that the depolarization of mitochondrial membranes was induced by H/R injury. CA pretreatment significantly increased JC-1 aggregation and restored MMP in H/R-injured IEC-6 cells (Fig. 3a). I/R injuries may lead to the disruption of mitochondrial respiration [56], with the

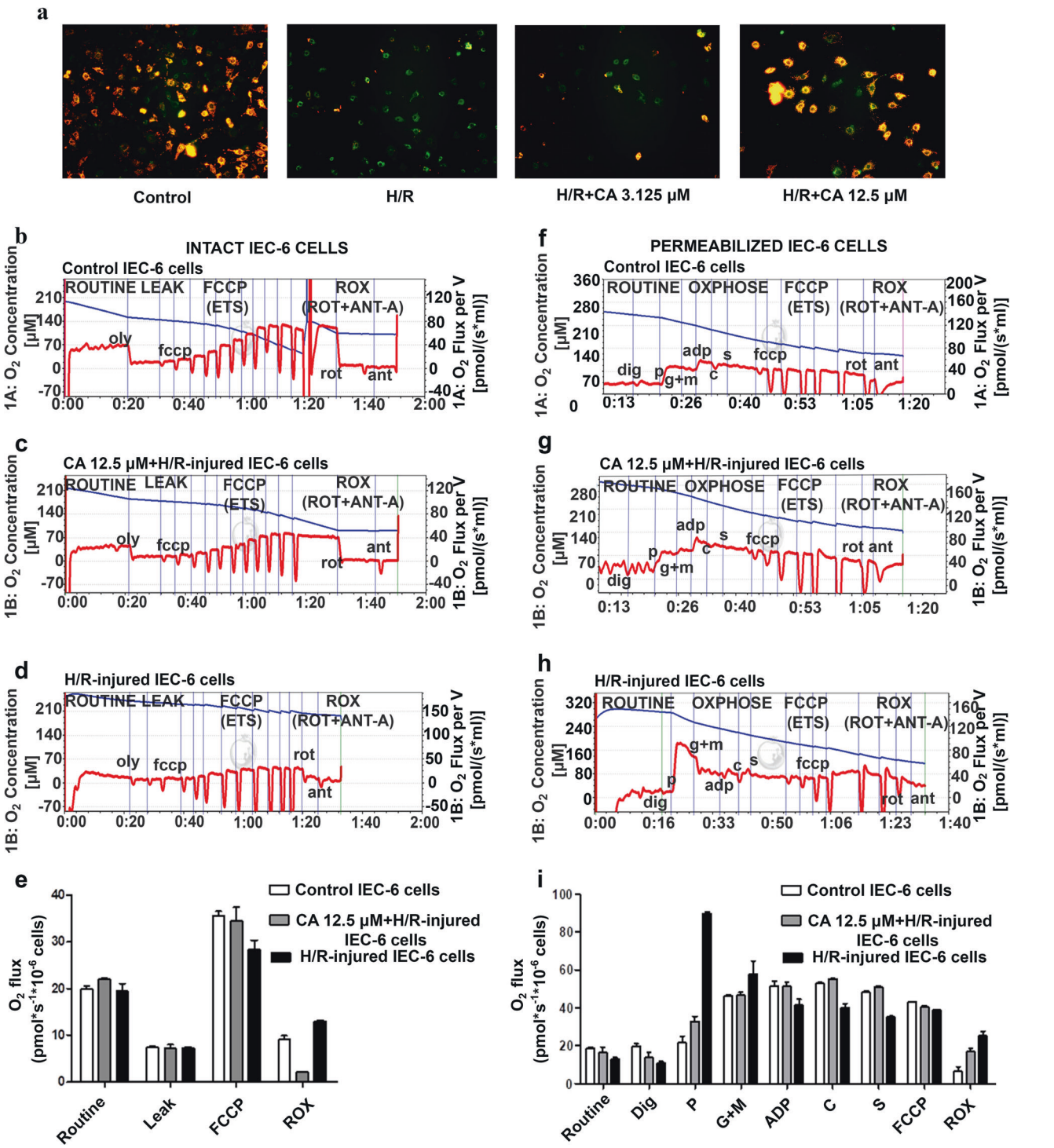

Fig. 3 Cinnamaldehyde improved mitochondrial respiration function and MMP ($\Delta\Psi m$) in H/R-injured IEC-6 cells. **a** Mitochondrial membrane potential (MMP $\Delta\Psi m$) assays were performed by using JC-1 staining in normal/H/R-injured IEC-6 cells. **b** Mitochondrial respiration of intact IEC-6 cells is shown; the plot of oxygen consumption flux per 1×10^6 cells in DMEM at 37 °C: control IEC-6 cells, (**c**) CA 12.5 μmol · L^{-1} + H/R-injured IEC-6 cells, and (**d**) H/R-injured IEC-6 cells. **e** Shown are the average basal respiration (ROUTINE), Oligomycin/Oly (LEAK), FCCP (maximal electron transport system ETS) and rotenone/Rot and Antimycin-A/ Ant-A (ROX). **f** Mitochondrial respiration of permeabilized IEC-6 is shown; the graph represents the plot of oxygen consumption flux per 1×10^6 cells in DMEM at 37 °C: control IEC-6 cells, (**g**) CA 12.5 μmol · L^{-1} + H/R-injured IEC-6 cells, and (**h**) H/R-injured IEC-6 cells. **i** Average values are shown for digitonin (Dig), pyruvate (P), glutamate (G) and malate (M), ADP, cytochrome-*c* (C), succinate (S), FFCP, rotenone (Rot) and antimycin-A (Ant-A)

impairment of maximal capacity of the electron transfer system (ETS) [57]. The results indicated that CA pretreatment significantly reversed the reduced ETS capacity in H/R-injured IEC-6 cells, which was characterized by improving mitochondrial respiration in intact cells (Fig. 3b-e). CA pretreatment also showed a significant elevation of ADP, cytochrome *c* and ETS compared with that of H/R-injured IEC-6 cells, indicating that CA-induced improvement of respiration in permeabilized H/R-injured IEC-6 cells (Fig. 3f-i)

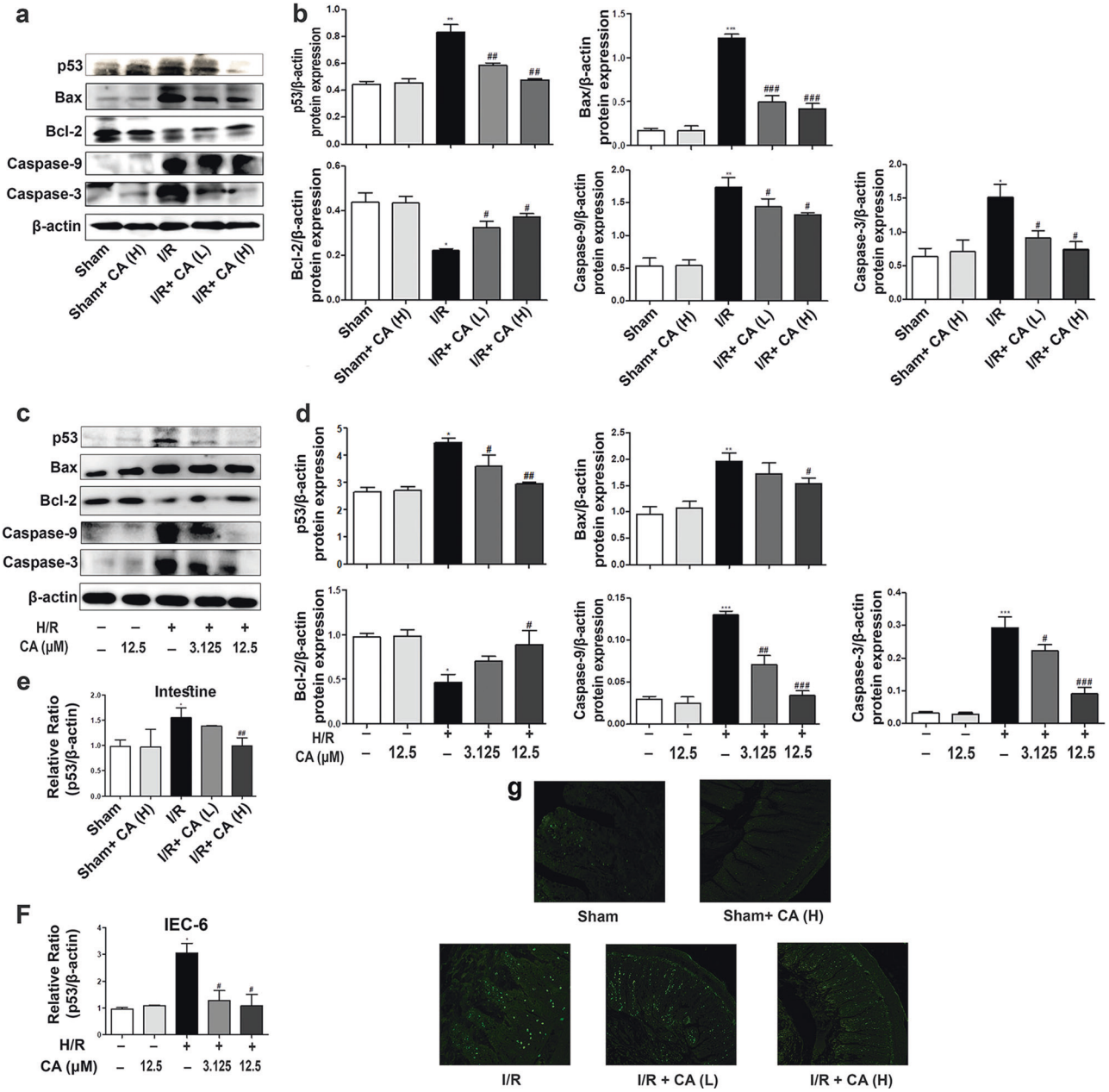

Fig. 4 Cinnamaldehyde ameliorated apoptosis in intestinal I/R-injuries and H/R injuries. **a** Apoptotic protein levels of Bax, Bcl-2, caspase-9, caspase-3, and p53 in sham-operated/I/R-injured intestinal tissues from three individual samples of randomly selected rats from each group. **b** Quantification analysis of apoptotic protein levels in intestinal tissues of three independent experiments. **c** The protein levels of Bax, Bcl-2, caspase-9, caspase-3, and p53 in 3 individual samples of normal/H/R-injured IEC-6. **d** Quantification analysis of apoptotic protein levels in three independent experiments for normal/H/R-injured IEC-6 cells. **e** p53 mRNA levels in intestinal tissues. **f** p53 mRNA levels in normal/H/R-injured IEC-6 cells. **g** TUNEL staining in intestinal I/R-injured tissues (All images original magnification ×200). Data are expressed as the mean ± SD ($n = 3$), $^{***}P < 0.001$, $^{**}P < 0.01$, and $^{*}P < 0.05$ vs control group; $^{###}P < 0.001$, $^{##}P < 0.01$, and $^{#}P < 0.05$ vs I/R group

and suggesting that the CA-reduced H/R injuries were related to the mitigation of mitochondrial respiration dysfunction.

Role of p53 and NF-κB in cinnamaldehyde-induced amelioration

Inhibitory effects of cinnamaldehyde on P53. P53 is found to play a transcriptional role in the nucleus [58], and it mediates inflammation, oxidative stress, and apoptosis in cell and tissue injuries [59–61]. P53 is the main member of the p53-dependent apoptotic family [62]. Our results obtained from Western blot analysis indicated that expression of apoptosis regulatory proteins, including Bax, caspase-9, caspase-3, and p53, was significantly upregulated, and Bcl-2 expression was significantly downregulated in both I/R-injured rats and H/R-injured IEC-6 cells compared with that of the corresponding normal controls. CA pretreatment significantly reversed not only the increased expression of Bax, caspase-9, caspase-3, and p53 but also reversed the decreased expression of Bcl-2 in both I/R-injured rats and H/R-injured IEC-6 cells, indicating that CA protected against intestinal I/R-induced apoptosis (Fig. 4a-d). The results obtained using RT-qPCR indicated that p53 gene expression was significantly upregulated in both I/R-injured rats and H/R-injured IEC-6 cells, and CA pretreatment significantly reversed the upregulation of p53 gene in both I/R-injured rats and H/R-injured cells (Fig. 4e, f), suggesting that the CA-mediated reduction in injuries was related

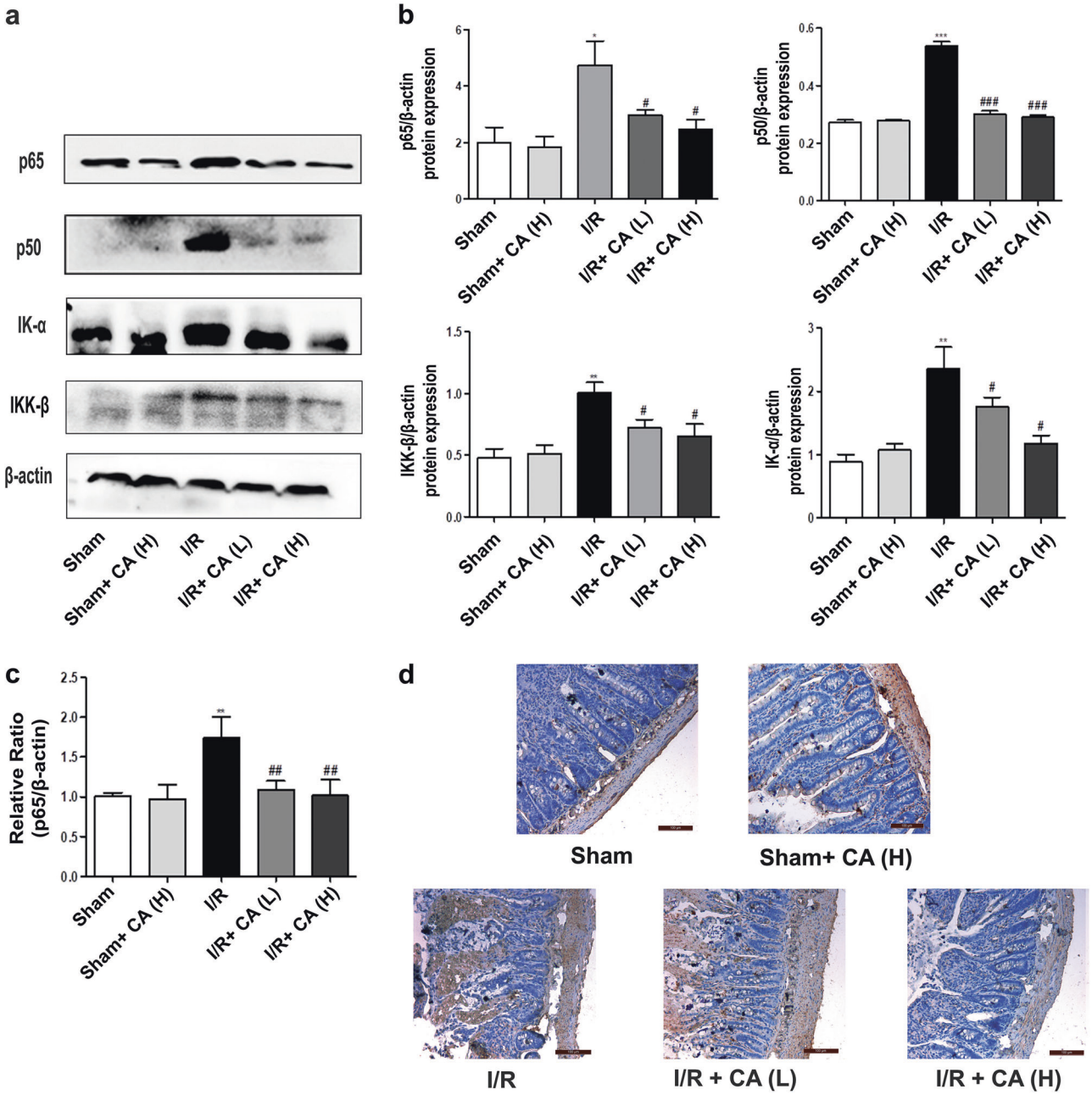

Fig. 5 Cinnamaldehyde protected against intestinal I/R injuries through inhibition of NF-κB in rats. **a** Protein levels of IKKβ, IK-α, NF-κB p50, and NF-κB p65 in the intestinal tissues from three individual samples of randomly selected rats from each group. **b** Quantification analysis of NF-κB-related proteins in the intestinal tissues from three independent experiments. **c** NF-κB p65 mRNA levels in intestinal tissues. **d** Immunohistochemical staining of NF-κB p65 in I/R-injured rats (original image magnification ×200). Data are expressed as the mean ± SD ($n = 3$), $^{***}P < 0.001$, $^{**}P < 0.01$, and $^{*}P < 0.05$ vs sham group; $^{###}P < 0.001$, $^{##}P < 0.01$, and $^{#}P < 0.05$ vs I/R group

to the decrease in apoptosis. CA did not significantly affect the gene expression in sham-operated rats or in normal IEC-6 cells.

Apoptotic TUNEL-positive cells were increased in I/R-injured rats compared with sham-operated rats. CA pretreatment (10 and 40 mg/kg) significantly decreased the number of TUNEL-positive cells in the villi of the intestine compared with that of the control I/R rats (Fig. 4g). These results also indicated that CA pretreatment significantly ameliorated intestinal I/R-induced apoptosis.

Inhibitory effects of cinnamaldehyde on NF-κB. NF-κB also plays an important role in tissue injuries [63, 64] and the related inflammation, immune responses [65], and apoptosis [66]. The NF-κB p65 subunit is the main member of the NF-κB transcription factor complex (which contains IKKβ, IK-α, NF-κB p50, and NF-κB p65) [67]. Western blot analysis indicated that expression of NF-κB-related proteins IKKβ, IK-α, NF-κB p50, and NF-κB p65 was significantly upregulated in both I/R-injured rats and H/R-injured IEC-6 cells compared with that of the corresponding normal controls. CA pretreatment significantly downregulated IKKβ, IK-α, NF-κB p50, and NF-κB p65 expressions in both I/R-injured rats (Fig. 5a, b) and H/R-injured IEC-6 cells (Fig. 6a, b). The results obtained using RT-qPCR indicated that NF-κB p65 gene expression was significantly upregulated in both I/R-injured rats and H/R-injured IEC-6 cells, and CA pretreatment significantly reversed the upregulation of NF-κB p65 in treated I/R-injured rats (Fig. 5c) and treated H/R-injured IEC-6 cells (Fig. 6c); these results indicate that

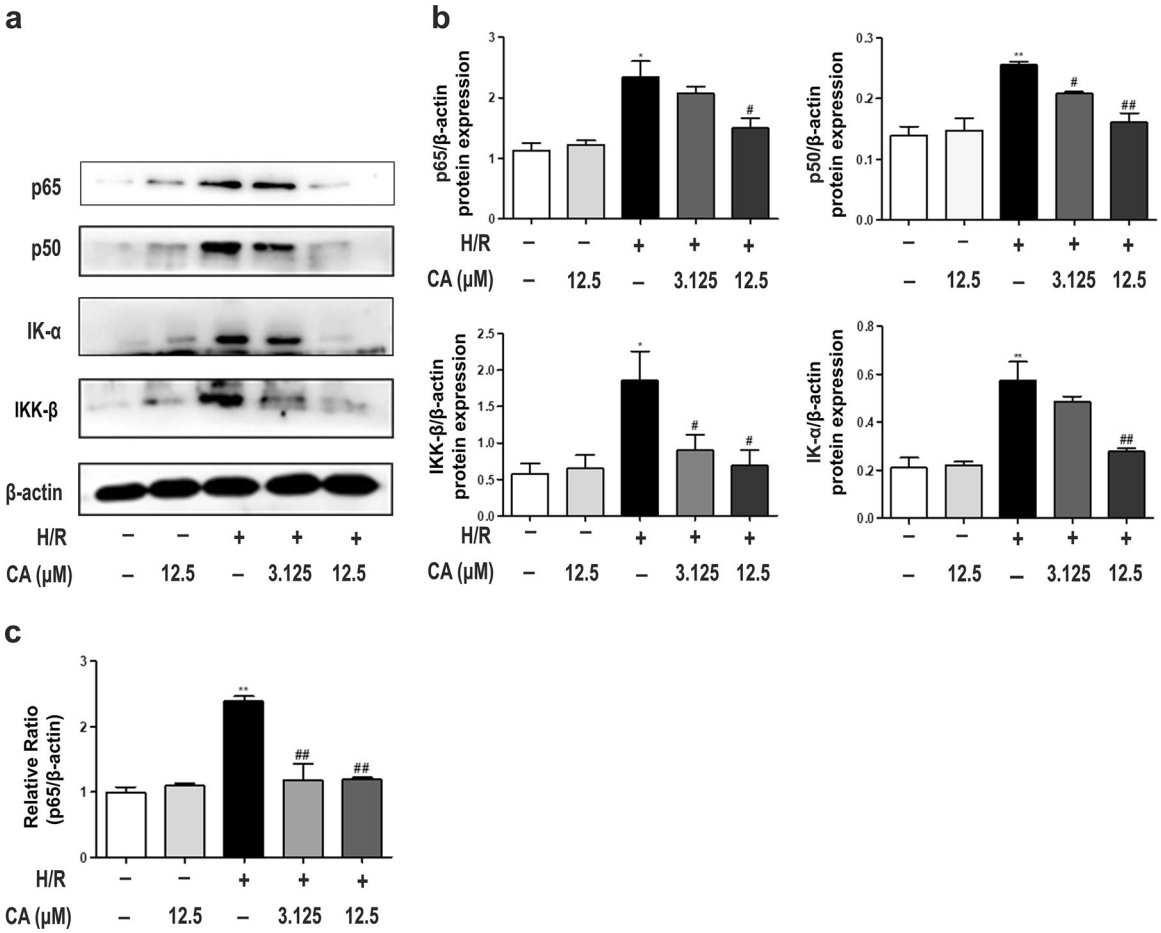

Fig. 6 Cinnamaldehyde protected against H/R injuries through inhibition of NF-κB in IEC-6 cells. **a** Protein levels of IKKβ, IK-α, NF-κB p50, and NF-κB p65 in three individual samples of normal/H/R-injured IEC-6 cells. **b** Quantification analysis of NF-κB-related proteins in three independent samples of normal/H/R-injured IEC-6 cells. **c** NF-κB p65 mRNA levels in normal/H/R-injured IEC-6 cells. Data are expressed as the mean ± SD ($n = 3$), $^{***}P < 0.001$, $^{**}P < 0.01$, and $^{*}P < 0.05$ vs sham group; $^{###}P < 0.001$, $^{##}P < 0.01$, and $^{#}P < 0.05$ vs H/R group

NF-κB p65 played an important role in CA ameliorated intestinal I/R- and H/R injuries. CA did not significantly affect gene expression in sham-operated rats or in normal IEC-6 cells.

Immunohistochemical analysis also showed that the increased protein expression of NF-κB p65 was observed in I/R-injured rats compared with the sham-operated rats. CA pretreatment also significantly reversed the increase in NF-κB p65 expression, confirming the role of NF-κB p65 in CA-induced amelioration. CA pretreatment did not significantly affect NF-κB p65 expression in the sham-operated rats (Fig. 5d).

Inhibitory effects of cinnamaldehyde on I/R-induced NF-κB p65 and p53 nuclear translocation. Both NF-κB p65 and p53 are transcriptional factors that remain inactive in the cytoplasm under an unstressed state, but stimuli can promote NF-κB p65 and p53 subunit translocation into the nucleus and trigger the release of pro-inflammatory cytokines and proapoptotic genes [58, 68, 69]. Our immunofluorescence assays indicated that more translocated nuclear NF-κB p65 was observed in H/R-injured IEC-6 cells than was observed in the control of IEC-6 cells. CA pretreatment significantly inhibited the nuclear translocation of NF-κB p65 in H/R-injured IEC-6 cells in a dose-dependent manner (Fig. 7a), indicating the role of NF-κB p65 in CA-induced amelioration.

The immunofluorescence assays also indicated that more nuclear translocation of p53 expression was observed in H/R-injured IEC-6 cells than was observed in the control IEC-6 cells. CA pretreatment significantly inhibited the nuclear translocation of p53 in H/R-injured IEC-6 cells (Fig. 7b), confirming the role of p53 in CA-induced amelioration.

Cinnamaldehyde–induced inhibition of NF-κB p65 and p53 in a synergistic manner. NF-κB p65 and p53 are transcription factors that may induce the activation or inhibition of one another, suggesting a potential relationship and interaction between NF-κB and p53 [70–72]. NF-κB, p53, and Bax activation plays a crucial role in apoptosis [73–75]. The proapoptotic activity of p53 is promoted through stimulation of specific proapoptotic target genes such as Bax [75, 76]. Bax also plays an important role in NF-κB p65-mediated apoptosis [77]. The roles of NF-κB p65, p53, and Bax were evaluated in CA-induced amelioration of H/R injuries in the present study. H/R-injured IEC-6 cells were transfected with either an siRNA that knockdown or a cDNA that overexpressed NF-κB p65 and p53; transfections were performed for the siRNA and cDNA individually or in combination. The expression levels of NF-κB p65, p53, and Bax were determined to reveal the role of NF-κB and/or p53 activation in CA-induced amelioration of I/R injuries. The results indicated that the protein expression levels of Bax, NF-κB p65, and p53 were significantly decreased in all NF-κB p65 and/or p53 siRNA-transfected H/R-injured IEC-6 cells compared with that of the control siRNA-transfected H/R-injured IEC-6 cells. Bax protein expression was further decreased in the double knockdown of both p53 and NF-κB p65 and in the single knockdown of p53 compared with that of the NF-κB p65 single knockdown (Fig. 8a, b), indicating the important role of p53 in activating Bax.

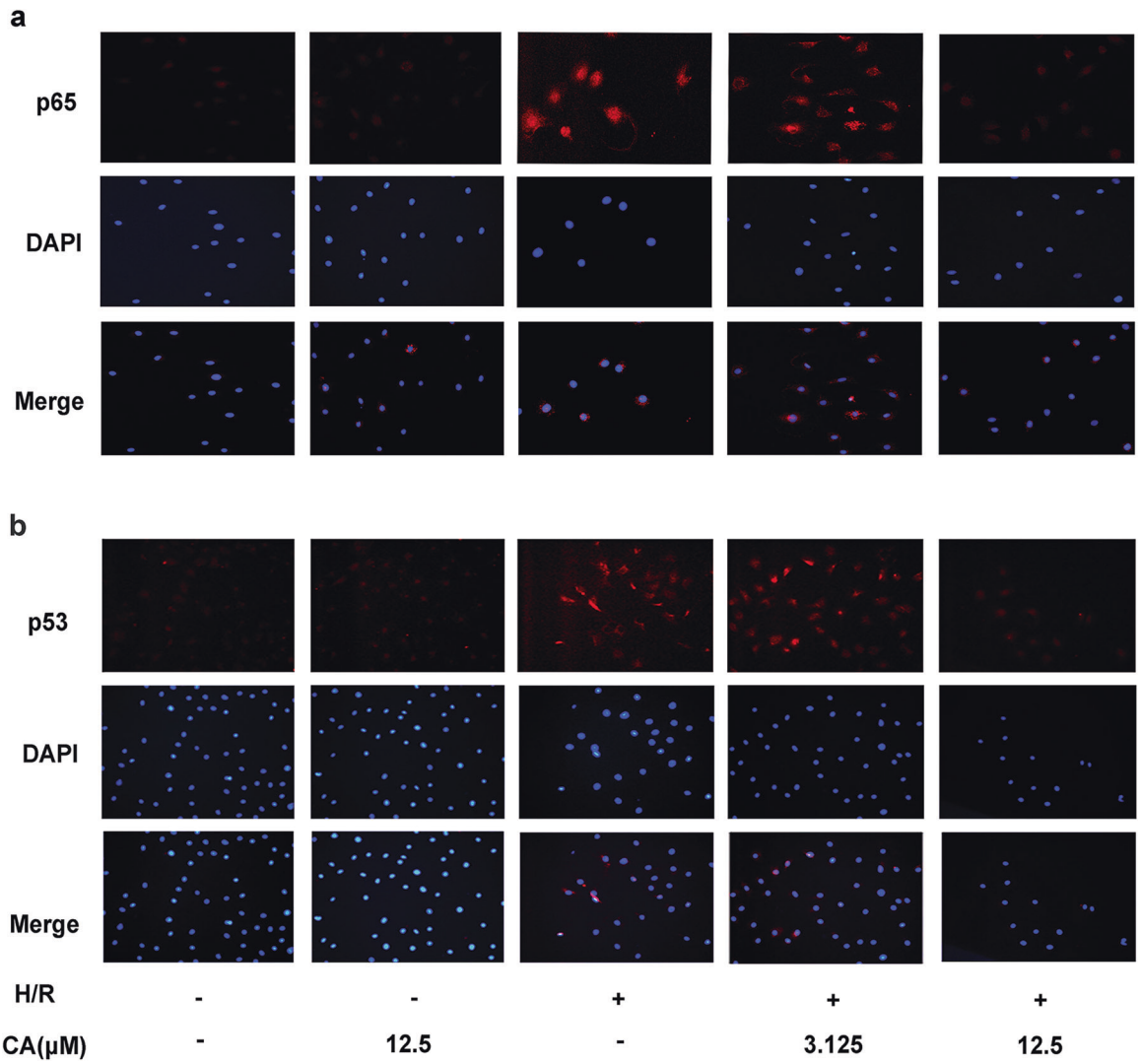

Fig. 7 Cinnamaldehyde inhibited NF-κB and p53 nuclear translocation in H/R-injured IEC-6 cells. **a** Immunofluorescence assay of NF-κB p65 in normal/H/R-injured IEC-6 cells. **b** Immunofluorescence assay of p53 in normal/H/R-injured IEC-6 cells

Double knockdown of NF-κB p65 and p53 did not further decrease NF-κB p65 expression compared with the levels in either of the single knockdown experiments (NF-κB p65 or p53), and p53 protein expression was significantly decreased following single p53 knockdown compared with that of the single NF-κB p65 knockdown; p53 levels further decreased following double knockdown compared with that of the single knockdown of NF-κB p65 or p53, indicating that p53 is activated by NF-κB in intestinal I/R injuries (Fig. 8c, d) and NF-κB p65 plays an important role in activating p53 in intestinal I/R injuries. CA pretreatment did not further reduce the protein expression of NF-κB p65 and p53 in siRNA NF-κB p65 and p53 cotransfected H/R-injured IEC-6 cells, indicating that NF-κB and p53 are the major targets for CA-induced amelioration of I/R and H/R injuries (Fig. 8c, d).

The protein expression levels of Bax, NF-κB p65, and p53 were significantly increased in all NF-κB p65- and/or p53 cDNA-transfected H/R-injured IEC-6 cells compared with control cDNA-transfected H/R-injured IEC-6 cells. The protein expression of Bax was further increased in the overexpression of both p53 and NF-κB p65 and in the overexpression of p53 alone compared with individual NF-κB p65 overexpression, indicating a role for p53 in promoting Bax activation (Fig. 8e, f). Dual overexpression of NF-κB p65 and p53 did not further increase NF-κB p65 expression over what was observed following overexpression of either NF-κB p65 or p53; further, p53 protein expression was significantly increased in single p53 overexpression experiments compared with that of single NF-κB p65 overexpression experiments, and p53 further increased in dual overexpression compared with that of the single overexpression of NF-κB p65 or p53. These results indicate that p53 is activated by NF-κB in intestinal I/R injuries (Fig. 8g, h), and NF-κB p65 plays an important role in activating p53 in intestinal I/R injuries. CA pretreatment could not decrease the protein expression of NF-κB p65 and p53 in H/R-injured IEC-6 cells that were cotransfected with the NF-κB p65 and p53 cDNAs, suggesting that NF-κB and p53 are the major targets for CA-induced amelioration of I/R and H/R injuries (Fig. 8g, h).

Immunoprecipitation assays were performed with a p53 antibody and were followed by immunoblotting for NF-κB p65, and they revealed the presence of an interaction between p53 and NF-κB p65. There was higher binding affinity between p53 and NF-κB p65 in H/R-injured IEC-6 cells than there was in CA + H/R-injured IEC-6 cells and normal IEC cells (Fig. 8i), showing the basis for CA-induced synergistic inhibition of p53 and NF-κB p65.

DISCUSSION

Tissue injuries, including those to liver [78], brain [79], heart [80], and intestine [81], are related to excessive/aberrant inflammation,

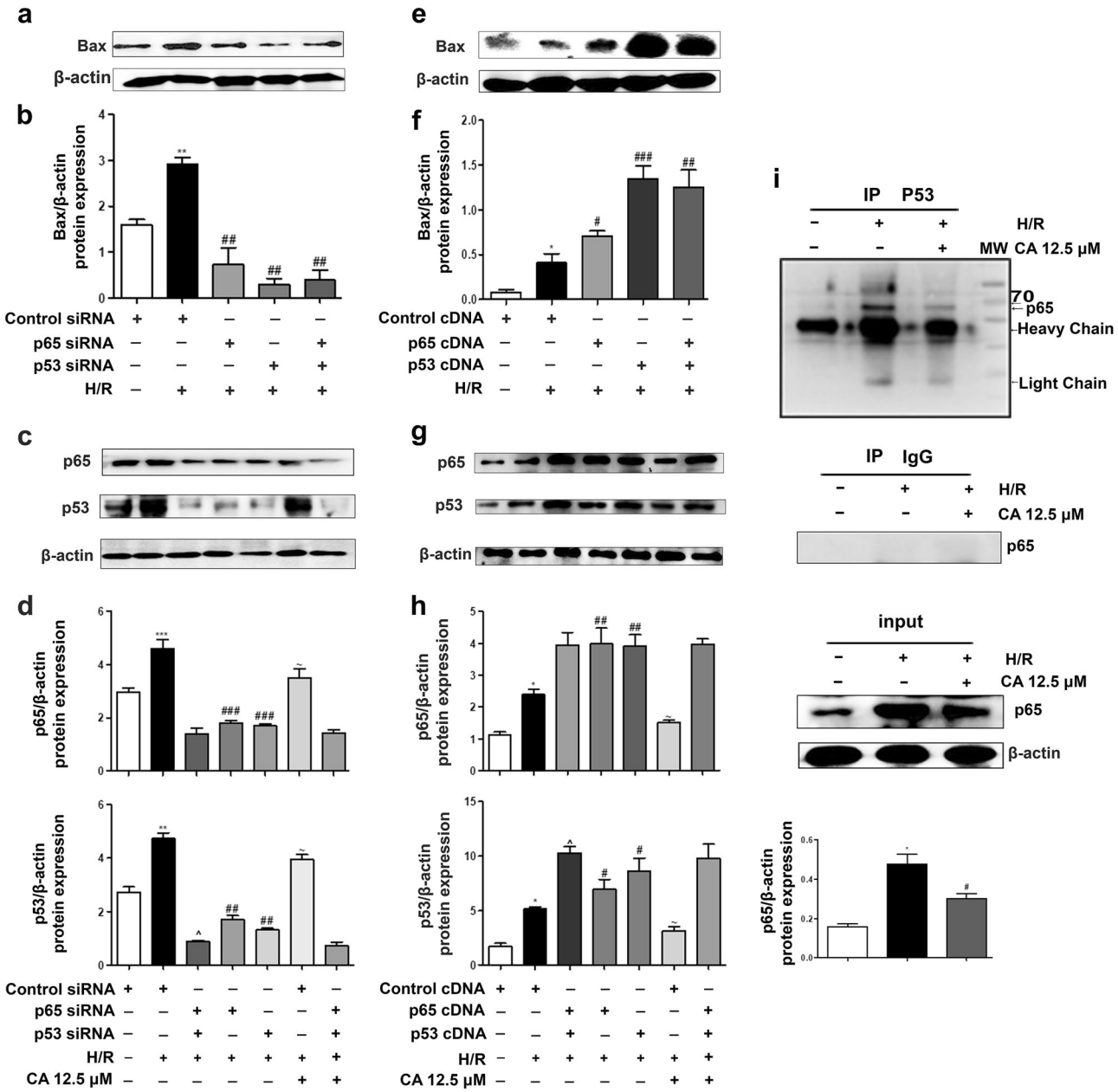

Fig. 8 Effects of cinnamaldehyde in NF-κB p65 + p53 siRNA and cDNA cotransfected IEC-6 cells. **a** Protein level of Bax in control siRNA-transfected IEC-6 cells, in control siRNA-transfected H/R-injured IEC-6 cells, in NF-κB p65 siRNA-transfected H/R-injured IEC-6 cells, in p53 siRNA-transfected H/R-injured IEC-6 cells, and in NF-κB p65 + p53 siRNA cotransfected H/R-injured IEC-6 cells. **b** Quantification analysis of the parameters in (**a**). **c** Protein levels of NF-κB p65 and p53 in control siRNA-transfected IEC-6 cells, in control siRNA-transfected H/R-injured IEC-6 cells, in NF-κB p65 siRNA-transfected H/R-injured IEC-6 cells, in p53 siRNA-transfected H/R-injured IEC-6 cells, in NF-κB p65 + p53 siRNA cotransfected H/R-injured IEC-6 cells, in control siRNA transfected and CA pretreated H/R-injured IEC-6 cells, and in CA pretreated and NF-κB p65 + p53 siRNA cotransfected H/R-injured IEC-6 cells. **d** Quantification analysis of the parameters in (**c**). **e** Protein level of Bax in control cDNA-transfected IEC-6 cells, in control cDNA-transfected H/R-injured IEC-6 cells, in NF-κB p65 cDNA-transfected H/R-injured IEC-6 cells, in p53 cDNA-transfected H/R-injured IEC-6 cells, and in NF-κB p65 + p53 cDNA cotransfected H/R-injured IEC-6 cells. **f** Quantification analysis of the parameters in (**e**). **g** Protein levels of NF-κB p65 and p53 in control cDNA-transfected IEC-6 cells, in control cDNA-transfected H/R-injured IEC-6 cells, in NF-κB p65 cDNA-transfected H/R-injured IEC-6 cells, in p53 cDNA-transfected H/R-injured IEC-6 cells, in NF-κB p65 + p53 cDNA cotransfected H/R-injured IEC-6 cells, in control cDNA-transfected and CA pretreated H/R-injured IEC-6 cells, and in CA pretreated and NF-κB p65 + p53 cDNA cotransfected H/R-injured IEC-6 cells. **h** Quantification analysis of the parameters in (**g**). **i** A p53 antibody was immunoprecipitated after incubation with extract from control IEC-6 cells, H/R-injured IEC-6 cells, and CA pretreated and H/R-injured IEC-6 cells; NF-κB p65 was used for immunoblotting. Data are expressed as the mean ± SD ($n = 3$), $^{***}P < 0.001$, $^{**}P < 0.01$, and $^{*}P < 0.05$ vs control siRNA or cDNA IEC-6 cells; $^{\#\#\#}P < 0.001$, $^{\#\#}P < 0.01$, and $^{\#}P < 0.05$ vs H/R + siRNA or cDNA IEC-6 cells; $^{\sim}P < 0.05$ vs protein expression before H/R in transfection with NF-κB p65 and p53; $^{\wedge}P < 0.05$ vs single transfection

oxidative stress, mitochondrial dysfunction, and apoptosis [82]. Mitochondria are known as the energy factory of cells [83], and inflammation, ROS generation, mitochondrial dysfunction, and apoptosis are also found in I/R injuries [84].

Our results obtained from both in vivo and in vitro studies support our hypothesis. CA pretreatment ameliorated severe I/R-induced morphological damage in rat intestinal tissues and reversed the injury-related functional/biochemical changes. CA

pretreatment significantly ameliorated I/R-induced inflammation by reducing infiltration of inflammatory cells and levels of pro-inflammatory cytokines (TNF-α, IL-1β, and IL-6) and by reducing neutrophil myeloperoxidase enzyme (MPO). CA pretreatment significantly ameliorated I/R- and H/R-induced oxidative stress by reversing SOD, GSH, LDH, and MDA levels in I/R-injured rats and by reducing ROS generation in H/R-injured IEC-6 cells. Our results also indicated that CA pretreatment significantly reversed the decreased MMP (ΔΨm) and significantly enhanced mitochondrial complexes in intact and permeabilized H/R-injured cells by enhancing ADP, cytochrome *c*, and ETS levels (Fig. 3), indicating that CA protected against intestinal I/R injuries at the mitochondrial level by improving mitochondrial respiration and reducing apoptosis. CA did not significantly affect the abovementioned parameters in the respective controls.

NF-κB and p53 are two main transcription factors involved in cell survival and cell division in response to genotoxic stimuli [85, 86]. NF-κB and its related proteins (IKKβ, IK-α, NF-κB p50, and NF-κB p65) play important roles in mediating inflammation and apoptosis [87]. The transcription factor p53 is the main p53 family member in the apoptotic signaling pathway [88, 89]. Activation of NF-κB or p53 plays a role in inducing inflammation, oxidative stress, and apoptosis in tissue injuries [90–92]. Myocardial I/R injuries are found to induce inflammation, oxidative stress, and apoptosis via the NF-κB pathway [93]. The p53 pathway also mediates cerebral and renal I/R-induced inflammation, oxidative stress, and apoptosis [94, 95]. Cerebral I/R injuries were also found to be mediated by both NF-κB and p53 pathways, resulting in excessive inflammation, oxidative stress, and apoptosis [96]. Our results revealed significant upregulation of NF-κB signaling pathway-related proteins, IKKβ, IK-α, NF-κB p50, and NF-κB p65, and significant upregulation of p53 signaling pathway-related proteins, Bax, caspase-9, caspase-3, and p53, and downregulation of Bcl-2, which were observed in both I/R and H/R injury conditions. CA pretreatment significantly reversed all these changes in I/R-injured rats and H/R-injured IEC-6 cells. CA pretreatment also significantly reduced the number of TUNEL-positive cells and significantly reduced NF-κB p65 expression in I/R-injured rats, revealing CA-induced amelioration of inflammation and apoptosis. The nuclear translocations of NF-κB p65 and p53 in different types of I/R injuries, including intestinal I/R injuries, result in inflammation and apoptosis [40, 97]. Our results indicated that CA inhibited both NF-κB p65 and p53 nuclear translocation in H/R-injured IEC-6 cells, suggesting that inhibition of nuclear translocation and inhibition of inflammation and apoptosis were involved in CA-induced protection against intestinal I/R injuries.

NF-κB and p53 are activated in response to stress stimuli, and their activation results in apoptosis through either synergistic or antagonistic relationships [98–100]. P53 plays an important role in activating Bax-induced apoptosis [101, 102]. Upon activation by oncogene-induced pathways or DNA damage, p53 promotes the expression of some proapoptotic genes that are involved in apoptosis, including Bax [75, 76]. Bax also plays a role in NF-κB-mediated apoptosis [103]. The NF-κB p65 subunit plays a key role in determining the duration, strength, and specificity of NF-κB-related gene programs [104–106], and p53 is a transcription factor that, of the p53-mediated genes, is known to be the main gene that functions in apoptosis [89, 107]. Our results indicated that the reduction of Bax expression in p53 siRNA-transfected H/R-injured IEC-6 cells was more significant compared with that of NF-κB p65-transfected H/R-injured IEC-6 cells, revealing the role of p53 in activating Bax and inducing apoptosis. Simultaneous knockdown of both NF-κB p65 and p53 protein expression did not result in a further decrease in NF-κB p65 protein expression over what was observed in either single knockdown (NF-κB p65 or p53). Further, simultaneous knockdown of NF-κB p65 and p53 resulted in the expression of p53 being reduced to levels that were lower than what was observed following knockdown of either NF-κB p65 or p53 individually in transfected cells, suggesting that NF-κB p65 promoted p53 activation during intestinal I/R injuries (Fig. 8). Additionally, CA pretreatment did not further reduce the protein expression of NF-κB p65 and p53 in siRNA NF-κB p65 and siRNA p53 cotransfected H/R-injured IEC-6 cells, indicating that NF-κB and p53 are the major targets for CA-induced amelioration and that simultaneous inhibition of NF-κB and p53 exerts a combined alleviation of I/R and H/R injuries. Overexpression of both NF-κB p65 and p53 together showed that p53 protein expression was further increased over what was observed following single overexpression of either NF-κB p65 or p53 in cDNA-transfected cells, suggesting that NF-κB p65 promoted p53 activation. Additionally, CA pretreatment could not reduce the protein expression of NF-κB p65 and p53 in cDNA NF-κB p65 and p53 cotransfected H/R-injured IEC-6 cells, indicating that CA-induced amelioration via synergistic inhibition of NF-κB and p53 activity in the conditions of I/R and H/R injuries.

The results from immunoprecipitation assays supported the presence of an interaction between p53 and NF-κB p65 and showed the basis for CA-induced amelioration via combined inhibition of NF-κB and p53 activity during I/R and H/R injuries.

Taken together, our in vivo and in vitro studies showed that CA pretreatment significantly protected against and ameliorated intestinal I/R and H/R injuries by improving mitochondrial function and reducing excessive inflammation, oxidative stress, and apoptosis. CA did not significantly affect the in vivo and in vitro normal controls. CA-induced synergistic inhibition of NF-κB and p53 plays a key role in protecting against and ameliorating intestinal I/R injuries. Our study suggests that CA can be considered a prophylactic drug for ameliorating I/R injuries, but the exact relationship between NF-κB and p53 under I/R conditions needs further study.

ACKNOWLEDGEMENTS

This study was supported by the National Natural Science Foundation of China (Grant No. 30772601, 81302838).

AUTHOR CONTRIBUTIONS

MA, JW, BX, YCS and MQL were responsible for the research design and performed the experiments; MA, YLL, EQ, MAA, AS, DPC and LW performed the data analysis; MA wrote the paper; YL and PYS guided the research.

ADDITIONAL INFORMATION

Competing interests The authors declare no competing interests.

REFERENCES

1. Ou-Yang L, Liu Y, Wang BY, Cao P, Zhang JJ, Huang YY, et al. Carnosine suppresses oxygen-glucose deprivation/recovery-induced proliferation and migration of reactive astrocytes of rats in vitro. Acta Pharmacol Sin. 2018;39:24–34.
2. Liu S, Yang Y, Song YQ, Geng J, Chen QL. Protective effects of N(2)LalanylLglutamine mediated by the JAK2/STAT3 signaling pathway on myocardial ischemia reperfusion. Mol Med Rep. 2018;17:5102–8.
3. Gao S, Zhu Y, Li H, Xia Z, Wu Q, Yao S, et al. Remote ischemic postconditioning protects against renal ischemia/reperfusion injury by activation of T-LAK-cell-originated protein kinase (TOPK)/PTEN/Akt signaling pathway mediated anti-oxidation and anti-inflammation. Int Immunopharmacol. 2016;38:395–401.
4. Gonul Y, Ozsoy M, Kocak A, Ozkececi ZT, Karavelioglu A, Bozkurt MF, et al. Antioxidant, antiapoptotic and inflammatory effects of interleukin-18 binding protein on kidney damage induced by hepatic ischemia reperfusion. Am J Med Sci. 2016;351:607–15.
5. Li Y, Feng D, Wang Z, Zhao Y, Sun R, Tian D, et al. Ischemia-induced ACSL4 activation contributes to ferroptosis-mediated tissue injury in intestinal ischemia/reperfusion. Cell Death Differ. 2019;26:2284–99.
6. Varga J, Toth S, Stasko P, Toth S Jr, Bilecova-Rabajdova M, Ostro A, et al. Intestinal ischemia-reperfusion injury—the histopathological status of remote vital organs in acute and subacute phases. Ann Transpl. 2012;17:11–20.

7. He XH, Li QW, Wang YL, Zhang ZZ, Ke JJ, Yan XT, et al. Transduced PEP-1-heme oxygenase-1 fusion protein reduces remote organ injury induced by intestinal ischemia/reperfusion. Med Sci Monit. 2015;21:1057–65.
8. Liu L, Yao J, Li Z, Zu G, Feng D, Li Y, et al. miR-381-3p knockdown improves intestinal epithelial proliferation and barrier function after intestinal ischemia/reperfusion injury by targeting nurr1. Cell Death Dis. 2018;9:411.
9. Wang Z, Ji Y, Wang S, Wang R, Li Z, Kang A, et al. Protective effect of intestinal ischemic preconditioning on ischemia reperfusion-caused lung injury in rats. Inflammation. 2015;38:424–32.
10. Iida T, Takagi T, Katada K, Mizushima K, Fukuda W, Kamada K, et al. Rapamycin improves mortality following intestinal ischemia-reperfusion via the inhibition of remote lung inflammation in mice. Digestion. 2015;92:211–9.
11. Yang X, Gao X, Du B, Zhao F, Feng X, Zhang H, et al. Ilex asprella aqueous extracts exert in vivo anti-inflammatory effects by regulating the NF-kappaB, JAK2/STAT3, and MAPK signaling pathways. J Ethnopharmacol. 2018;225:234–43.
12. Guo X, Cen Y, Wang J, Jiang H. CXCL10-induced IL-9 promotes liver fibrosis via Raf/MEK/ERK signaling pathway. Biomed Pharmacother. 2018;105:282–9.
13. Lu C, Li Y, Hu S, Cai Y, Yang Z, Peng K. Scoparone prevents IL-1beta-induced inflammatory response in human osteoarthritis chondrocytes through the PI3K/Akt/NF-kappaB pathway. Biomed Pharmacother. 2018;106:1169–74.
14. Scott AJ, Walker SA, Krank JJ, Wilkinson AS, Johnson KM, Lewis EM, et al. AIF promotes a JNK1-mediated cadherin switch independently of respiratory chain stabilization. J Biol Chem. 2018;293:14707–22.
15. Koyanagi M, Takahashi J, Arakawa Y, Doi D, Fukuda H, Hayashi H, et al. Inhibition of the Rho/ROCK pathway reduces apoptosis during transplantation of embryonic stem cell-derived neural precursors. J Neurosci Res. 2008;86:270–80.
16. Zhao D, Zhang M, Yuan H, Meng C, Zhang B, Wu H. Ginsenoside Rb1 protects against spinal cord ischemia-reperfusion injury in rats by downregulating the Bax/Bcl-2 ratio and caspase-3 and p-Ask-1 levels. Exp Mol Pathol. 2018;105:229–35.
17. Zhang XJ, He C, Tian K, Li P, Su H, Wan JB. Ginsenoside Rb1 attenuates angiotensin II-induced abdominal aortic aneurysm through inactivation of the JNK and p38 signaling pathways. Vasc Pharmacol. 2015;73:86–95.
18. Ma L, Mu Y, Zhang Z, Sun Q. Eugenol promotes functional recovery and alleviates inflammation, oxidative stress, and neural apoptosis in a rat model of spinal cord injury. Restor Neurol Neurosci. 2018;36:659–68.
19. Zhang LP, Jiang YC, Yu XF, Xu HI, Li M, Zhao XZ, et al. Ginsenoside Rg3 improves cardiac function after myocardial ischemia/reperfusion via attenuating apoptosis and inflammation. Evid Based Complement Altern Med. 2016;2016:6967853.
20. Lin Y, Sheng M, Ding Y, Zhang N, Song Y, Du H, et al. Berberine protects renal tubular cells against hypoxia/reoxygenation injury via the Sirt1/p53 pathway. J Nat Med. 2018;72:715–23.
21. Li S, Takahara T, Fujino M, Fukuhara Y, Sugiyama T, Li XK, et al. Astaxanthin prevents ischemia-reperfusion injury of the steatotic liver in mice. PloS ONE. 2017;12:e0187810.
22. Zhang W, Liu X, Jiang Y, Wang N, Li F, Xin H. 6-Gingerol attenuates ischemia-reperfusion-induced cell apoptosis in human AC16 cardiomyocytes through HMGB2-JNK1/2-NF-κB pathway. Evid Based Complement Altern Med. 2019;2019:8798653.
23. Yang X, Yue R, Zhang J, Zhang X, Liu Y, Chen C, et al. Gastrin protects against myocardial ischemia/reperfusion injury via activation of RISK (reperfusion injury salvage kinase) and SAFE (survivor activating factor enhancement) pathways. J Am Heart Assoc. 2018;7:e005171.
24. Guo J, Wang SB, Yuan TY, Wu YJ, Yan Y, Li L, et al. Coptisine protects rat heart against myocardial ischemia/reperfusion injury by suppressing myocardial apoptosis and inflammation. Atherosclerosis. 2013;231:384–91.
25. Chen YF, Wu KJ, Wood WG. Paeonia lactiflora extract attenuating cerebral ischemia and arterial intimal hyperplasia is mediated by paeoniflorin via modulation of VSMC migration and Ras/MEK/ERK signaling pathway. vid Based Complement Altern Med. 2013;2013:1–12.
26. Lian M, Sun Y, Lin Y, Wen J, Almoiliqy M, Xu B, et al. p-JAK2 plays a key role in catalpol-induced protection against rat intestinal ischemia/reperfusion injury. RSC Adv. 2017;7:54369–78.
27. Sun Y, Lian M, Lin Y, Xu B, Li Y, Wen J, et al. Role of p-MKK7 in myricetin-induced protection against intestinal ischemia/reperfusion injury. Pharmacol Res. 2018;129:432–42.
28. Wen J, Xu B, Sun Y, Lian M, Li Y, Lin Y, et al. Paeoniflorin protects against intestinal ischemia/reperfusion by activating LKB1/AMPK and promoting autophagy. Pharmacol Res. 2019;146:104308.
29. Zhao H, Yang Q, Xie Y, Sun J, Tu H, Cao W, et al. Simultaneous determination of cinnamaldehyde and its metabolite in rat tissues by gas chromatography–mass spectrometry. Biomed Chromatogr. 2015;29:182–7.
30. Mousavi F, Bojko B, Bessonneau V, Pawliszyn J. Cinnamaldehyde characterization as an antibacterial agent toward E. coli metabolic profile using 96-blade solid-phase microextraction coupled to liquid chromatography–mass spectrometry. J Proteome Res. 2016;15:963–75.
31. Kang LL, Zhang DM, Ma CH, Zhang JH, Jia KK, Liu JH, et al. Cinnamaldehyde and allopurinol reduce fructose-induced cardiac inflammation and fibrosis by attenuating CD36-mediated TLR4/6-IRAK4/1 signaling to suppress NLRP3 inflammasome activation. Sci Rep. 2016;6:27460.
32. Subash-Babu P, Alshatwi AA, Ignacimuthu S. Beneficial antioxidative and antiperoxidative effect of cinnamaldehyde protect streptozotocin-induced pancreatic β-cells damage in wistar rats. Biomol Ther (Seoul). 2014;22:47.
33. Lv C, Yuan X, Zeng H-W, Liu R-H, Zhang W-D. Protective effect of cinnamaldehyde against glutamate-induced oxidative stress and apoptosis in PC12 cells. Eur J Pharmacol. 2017;815:487–94.
34. Shen S, Zhang T, Yuan Y, Lin S, Xu J, Ye H. Effects of cinnamaldehyde on Escherichia coli and Staphylococcus aureus membrane. Food Control. 2015;47:196–202.
35. Muhammad JS, Zaidi SF, Shaharyar S, Refaat A, Usmanghani K, Saiki I, et al. Anti-inflammatory effect of cinnamaldehyde in Helicobacter pylori induced gastric inflammation. Biol Pharmacol Bull. 2015;38:109–15.
36. Babu PS, Prabuseenivasan S, Ignacimuthu S. Cinnamaldehyde—a potential antidiabetic agent. Phytomedicine. 2007;14:15–22.
37. Yang L, Wu QQ, Liu Y, Hu ZF, Bian ZY, Tang QZ. Cinnamaldehyde attenuates pressure overload-induced cardiac hypertrophy. Int J Clin Exp Pathol. 2015;8:14345.
38. Song F, Li H, Sun J, Wang S. Protective effects of cinnamic acid and cinnamic aldehyde on isoproterenol-induced acute myocardial ischemia in rats. J Ethnopharmacol. 2013;150:125–30.
39. Chen YF, Wang YW, Huang WS, Lee MM, Wood WG, Leung YM, et al. Trans-cinnamaldehyde, an essential oil in cinnamon powder, ameliorates cerebral ischemia-induced brain injury via inhibition of neuroinflammation through attenuation of iNOS, COX-2 expression and NF-κB signaling pathway. Neuromol Med. 2016;18:322–33.
40. Li Y, Xu B, Xu M, Chen D, Xiong Y, Lian M, et al. 6-Gingerol protects intestinal barrier from ischemia/reperfusion-induced damage via inhibition of p38 MAPK to NF-κB signalling. Pharmacol Res. 2017;119:137–48.
41. Liu Z, Jiang J, Yang Q, Xiong Y, Zou D, Yang C, et al. MicroRNA-682-mediated downregulation of PTEN in intestinal epithelial cells ameliorates intestinal ischemia–reperfusion injury. Cell Death Dis. 2016;7:e2210.
42. Chiu C-J, McArdle AH, Brown R, Scott HJ, Gurd FN. Intestinal mucosal lesion in low-flow states: I. A morphological, hemodynamic, and metabolic reappraisal. Arch Surg. 1970;101:478–83.
43. Gnaiger E, Steinlechner-Maran R, Méndez G, Eberl T, Margreiter R. Control of mitochondrial and cellular respiration by oxygen. J Bioenerg Biomembr. 1995;27:583–96.
44. Pesta D, Gnaiger E. High-resolution respirometry: OXPHOS protocols for human cells and permeabilized fibers from small biopsies of human muscle. Methods Mol Biol. 2012;810:25–58.
45. Wu H, Liu L, Tan Q, Wang C, Guo M, Xie Y, et al. Somatostatin limits intestinal ischemia-reperfusion injury in macaques via suppression of TLR4-NF-κB cytokine pathway. J Gastrointest Surg. 2009;13:983–93.
46. He X, Zheng Y, Liu S, Shi S, Liu Y, He Y, et al. MiR-146a protects small intestine against ischemia/reperfusion injury by down-regulating TLR4/TRAF6/NF-κB pathway. J Cell Physiol. 2018;233:2476–88.
47. Zu G, Guo J, Che N, Zhou T, Zhang X, Wang G, et al. Protective effects of ginsenoside Rg1 on intestinal ischemia/reperfusion injury-induced oxidative stress and apoptosis via activation of the Wnt/β-catenin pathway. Sci Rep. 2016;6:38480.
48. Liu HN, Guo NN, Guo WW, Huang-Fu MY, Vakili MR, Chen JJ, et al. Delivery of mitochondriotropic doxorubicin derivatives using self-assembling hyaluronic acid nanocarriers in doxorubicin-resistant breast cancer. Acta Pharmacol Sin. 2018;39:1681–92.
49. Krupkova O, Handa J, Hlavna M, Klasen J, Ospelt C, Ferguson SJ, et al. The natural polyphenol epigallocatechin gallate protects intervertebral disc cells from oxidative stress. Oxid Med Cell Longev. 2016;2016:7031397.
50. Chung HK, Rathor N, Wang SR, Wang JY, Rao JN. RhoA enhances store-operated Ca^{2+} entry and intestinal epithelial restitution by interacting with TRPC1 after wounding. Am J Physiol Gastrointest Liver Physiol. 2015;309:G759–67.
51. Huang BX, Kim HY. Effective identification of Akt interacting proteins by two-step chemical crosslinking, co-immunoprecipitation and mass spectrometry. PloS ONE. 2013;8:e61430.
52. Alam R, Schultz CR, Golembieski WA, Poisson LM, Rempel SA. PTEN suppresses SPARC-induced pMAPKAPK2 and inhibits SPARC-induced Ser78 HSP27 phosphorylation in glioma. Neuro Oncol. 2013;15:451–61.

53. Crane JD, Ogborn DI, Cupido C, Melov S, Hubbard A, Bourgeois JM, et al. Massage therapy attenuates inflammatory signaling after exercise-induced muscle damage. Sci Transl Med. 2012;4:119ra13.
54. Bellanti F, Mirabella L, Mitarotonda D, Blonda M, Tamborra R, Cinnella G, et al. Propofol but not sevoflurane prevents mitochondrial dysfunction and oxidative stress by limiting HIF-1α activation in hepatic ischemia/reperfusion injury. Free Radic Biol Med. 2016;96:323–33.
55. Liu XR, Cao L, Li T, Chen LL, Yu YY, Huang WJ, et al. Propofol attenuates H_2O_2-induced oxidative stress and apoptosis via the mitochondria-and ER-medicated pathways in neonatal rat cardiomyocytes. Apoptosis. 2017;22:639–46.
56. Rossetti A, Togliatto G, Rolo AP, Teodoro JS, Granata R, Ghigo E, et al. Unacylated ghrelin prevents mitochondrial dysfunction in a model of ischemia/reperfusion liver injury. Cell Death Disco. 2017;3:17077.
57. Hals IK, Bruerberg SG, Ma Z, Scholz H, Björklund A, Grill V. Mitochondrial respiration in insulin-producing β-cells: general characteristics and adaptive effects of hypoxia. PloS ONE. 2015;10:e0138558.
58. Kang R, Kroemer G, Tang D. The tumor suppressor protein p53 and the ferroptosis network. Free Radic Biol Med. 2019;133:162–8.
59. Chtourou Y, Aouey B, Kebieche M, Fetoui H. Protective role of naringin against cisplatin induced oxidative stress, inflammatory response and apoptosis in rat striatum via suppressing ROS-mediated NF-κB and P53 signaling pathways. Chem-Biol Interact. 2015;239:76–86.
60. Komarova EA, Krivokrysenko V, Wang K, Neznanov N, Chernov MV, Komarov PG, et al. p53 is a suppressor of inflammatory response in mice. FASEB J. 2005;19:1030–2.
61. Italiano D, Lena AM, Melino G, Candi E. Identification of NCF2/p67phox as a novel p53 target gene. Cell Cycle. 2012;11:4589–96.
62. Aubrey BJ, Strasser A, Kelly GL. Tumor-suppressor functions of the TP53 pathway. Cold Spring Harb Perspect Med. 2016;6: pii: a026062. https://doi.org/10.1101/cshperspect.a026062.
63. Xie YL, Chu JG, Jian XM, Dong JZ, Wang LP, Li GX, et al. Curcumin attenuates lipopolysaccharide/d-galactosamine-induced acute liver injury by activating Nrf2 nuclear translocation and inhibiting NF-kappaB activation. Biomed Pharmacother. 2017;91:70–7.
64. Kim JE, Lee MH, Nam DH, Song HK, Kang YS, Lee JE, et al. Celastrol, an NF-κB inhibitor, improves insulin resistance and attenuates renal injury in db/db mice. PloS ONE. 2013;8:e62068.
65. Liu T, Zhang L, Joo D, Sun SC. NF-kappaB signaling in inflammation. Signal Transduct Target Ther. 2017;2: pii: 17023. https://doi.org/10.1038/sigtrans.2017.23.
66. DiDonato JA, Mercurio F, Karin M. NF-kappaB and the link between inflammation and cancer. Immunol Rev. 2012;246:379–400.
67. Giridharan S, Srinivasan M. Mechanisms of NF-kappaB p65 and strategies for therapeutic manipulation. J Inflamm Res. 2018;11:407–19.
68. Sero JE, Sailem HZ, Ardy RC, Almuttaqi H, Zhang T, Bakal C. Cell shape and the microenvironment regulate nuclear translocation of NF-κB in breast epithelial and tumor cells. Mol Syst Biol. 2015;11:790.
69. Chipuk JE, Bouchier-Hayes L, Kuwana T, Newmeyer DD, Green DR. PUMA couples the nuclear and cytoplasmic proapoptotic function of p53. Science. 2005;309:1732–5.
70. Schneider G, Kramer OH. NFkappaB/p53 crosstalk-a promising new therapeutic target. Biochim Biophys Acta. 2011;1815:90–103.
71. Ryan KM, Ernst MK, Rice NR, Vousden KH. Role of NF-kappaB in p53-mediated programmed cell death. Nature. 2000;404:892–7.
72. Webster GA, Perkins ND. Transcriptional cross talk between NF-κB and p53. Mol Cell Biol. 1999;19:3485–95.
73. Perkins ND. NF-κB: tumor promoter or suppressor? Trends Cell Biol. 2004;14:64–9.
74. Yin M, Ren X, Zhang X, Luo Y, Wang G, Huang K, et al. Selective killing of lung cancer cells by miRNA-506 molecule through inhibiting NF-κB p65 to evoke reactive oxygen species generation and p53 activation. Oncogene. 2015;34:691.
75. Follis AV, Llambi F, Merritt P, Chipuk JE, Green DR, Kriwacki RW. Pin1-induced proline isomerization in cytosolic p53 mediates BAX activation and apoptosis. Mol Cell. 2015;59:677–84.
76. Chipuk JE, Kuwana T, Bouchier-Hayes L, Droin NM, Newmeyer DD, Schuler M, et al. Direct activation of Bax by p53 mediates mitochondrial membrane permeabilization and apoptosis. Science. 2004;303:1010–4.
77. Khandelwal N, Simpson J, Taylor G, Rafique S, Whitehouse A, Hiscox J, et al. Nucleolar NF-kappaB/RelA mediates apoptosis by causing cytoplasmic relocalization of nucleophosmin. Cell Death Differ. 2011;18:1889–903.
78. Bavarsad K, Riahi MM, Saadat S, Barreto G, Atkin SL, Sahebkar A. Protective effects of curcumin against ischemia-reperfusion injury in the liver. Pharmacol Res. 2019;141:53–62.
79. Liu YR, Li PW, Suo JJ, Sun Y, Zhang BA, Lu H, et al. Catalpol provides protective effects against cerebral ischaemia/reperfusion injury in gerbils. J Pharmacol Pharmacol. 2014;66:1265–70.
80. Pashkow FJ. Oxidative stress and inflammation in heart disease: do antioxidants have a role in treatment and/or prevention? Int J Inflam. 2011;2011:514623.
81. Wang G, Yao J, Li Z, Zu G, Feng D, Shan W, et al. miR-34a-5p inhibition alleviates intestinal ischemia/reperfusion-induced reactive oxygen species accumulation and apoptosis via activation of SIRT1 signaling. Antioxid Redox Signal. 2016;24:961–73.
82. Chen S, Li X, Wang Y, Mu P, Chen C, Huang P, et al. Ginsenoside Rb1 attenuates intestinal ischemia/reperfusioninduced inflammation and oxidative stress via activation of the PI3K/Akt/Nrf2 signaling pathway. Mol Med Rep. 2019;19:3633–41.
83. Claiborne AB, English RA, Kahn JP. Finding an ethical path forward for mitochondrial replacement. Science. 2016;351:668–70.
84. Wang Y, Liu J, Ma A, Chen Y. Cardioprotective effect of berberine against myocardial ischemia/reperfusion injury via attenuating mitochondrial dysfunction and apoptosis. Int J Clin Exp Med. 2015;8:14513.
85. Taniguchi K, Karin M. NF-κB, inflammation, immunity and cancer: coming of age. Nat Rev Immunol. 2018;18:309–24.
86. Bisio A, Zámborszky J, Zaccara S, Lion M, Tebaldi T, Sharma V, et al. Cooperative interactions between p53 and NFκB enhance cell plasticity. Oncotarget. 2014;5:12111.
87. Hoesel B, Schmid JA. The complexity of NF-kappaB signaling in inflammation and cancer. Mol Cancer. 2013;12:86.
88. Pietsch EC, Sykes SM, McMahon SB, Murphy ME. The p53 family and programmed cell death. Oncogene. 2008;27:6507–21.
89. Joerger AC, Fersht AR. The p53 pathway: origins, inactivation in cancer, and emerging therapeutic approaches. Annu Rev Biochem. 2016;85:375–404.
90. Kim HJ, Joe Y, Yu JK, Chen Y, Jeong SO, Mani N, et al. Carbon monoxide protects against hepatic ischemia/reperfusion injury by modulating the miR-34a/SIRT1 pathway. Biochim Biophys Acta Mol Basis Dis. 2015;1852:1550–9.
91. Plesnila N, von Baumgarten L, Retiounskaia M, Engel D, Ardeshiri A, Zimmermann R, et al. Delayed neuronal death after brain trauma involves p53-dependent inhibition of NF-kappaB transcriptional activity. Cell Death Differ. 2007;14:1529–41.
92. Zhang C, Liao P, Liang R, Zheng X, Jian J. Epigallocatechin gallate prevents mitochondrial impairment and cell apoptosis by regulating miR-30a/p53 axis. Phytomedicine. 2019;61:152845.
93. Li J, Xie C, Zhuang J, Li H, Yao Y, Shao C, et al. Resveratrol attenuates inflammation in the rat heart subjected to ischemia-reperfusion: role of the TLR4/NF-κB signaling pathway. Mol Med Rep. 2015;11:1120–6.
94. Chai YS, Hu J, Lei F, Wang YG, Yuan ZY, Lu X, et al. Effect of berberine on cell cycle arrest and cell survival during cerebral ischemia and reperfusion and correlations with p53/cyclin D1 and PI3K/Akt. Eur J Pharmacol. 2013;708:44–55.
95. Sutton TA, Wilkinson J, Mang HE, Knipe NL, Plotkin Z, Hosein M, et al. p53 regulates renal expression of HIF-1{alpha} and pVHL under physiological conditions and after ischemia-reperfusion injury. Am J Physiol Ren Physiol. 2008;295:F1666–77.
96. Cui DR, Wang L, Jiang W, Qi AH, Zhou QH, Zhang XL. Propofol prevents cerebral ischemia-triggered autophagy activation and cell death in the rat hippocampus through the NF-kappaB/p53 signaling pathway. Neuroscience. 2013;246:117–32.
97. Li XQ, Yu Q, Chen FS, Tan WF, Zhang ZL, Ma H. Inhibiting aberrant p53-PUMA feedback loop activation attenuates ischaemia reperfusion-induced neuroapoptosis and neuroinflammation in rats by downregulating caspase 3 and the NF-κB cytokine pathway. J Neuroinflammation. 2018;15:250.
98. Tanaka T, Tsuchiya R, Hozumi Y, Nakano T, Okada M, Goto K. Reciprocal regulation of p53 and NF-κB by diacylglycerol kinase ζ. Adv Biol Regul. 2016;60:15–21.
99. Meley D, Spiller DG, White MR, McDowell H, Pizer B, See V. p53-mediated delayed NF-kappaB activity enhances etoposide-induced cell death in medulloblastoma. Cell Death Dis. 2010;1:e41.
100. Ak P, Levine AJ. p53 and NF-κB: different strategies for responding to stress lead to a functional antagonism. FASEB J. 2010;24:3643–52.
101. Liao JM, Cao B, Deng J, Zhou X, Strong M, Zeng S, et al. TFIIS.h, a new target of p53, regulates transcription efficiency of pro-apoptotic bax gene. Sci Rep. 2016;6:23542.
102. Dashzeveg N, Yoshida K. Cell death decision by p53 via control of the mitochondrial membrane. Cancer Lett. 2015;367:108–12.
103. Mohan S, Abdelwahab SI, Kamalidehghan B, Syam S, May KS, Harmal NS, et al. Involvement of NF-kappaB and Bcl2/Bax signaling pathways in the apoptosis of

MCF7 cells induced by a xanthone compound Pyranocycloartobiloxanthone A. Phytomedicine. 2012;19:1007–15.
104. Hayden MS, Ghosh S. NF-kappaB, the first quarter-century: remarkable progress and outstanding questions. Genes Dev. 2012;26:203–34.
105. Oeckinghaus A, Hayden MS, Ghosh S. Crosstalk in NF-kappaB signaling pathways. Nat Immunol. 2011;12:695–708.
106. Kwon HJ, Choi GE, Ryu S, Kwon SJ, Kim SC, Booth C, et al. Stepwise phosphorylation of p65 promotes NF-κB activation and NK cell responses during target cell recognition. Nat Commun. 2016;7:11686.
107. Aubrey BJ, Kelly GL, Janic A, Herold MJ, Strasser A. How does p53 induce apoptosis and how does this relate to p53-mediated tumour suppression? Cell Death Differ. 2018;25:104.